Journal of Materials Science: Materials in Electronics (2018) 29:16864–16871
https://doi.org/10.1007/s10854-018-9781-x

Effects of Ta_2O_5 addition on relaxation behavior and electric properties of PMS–PNN–PZT ceramics

Hong-Wei Zhu[1] · De-Yi Zheng[2] · Xue-Jie Wang[1,3] · Liu Yang[2] · Chao Fang[2] · Ze-Hui Peng[2]

Received: 28 June 2018 / Accepted: 30 July 2018 / Published online: 3 August 2018

Abstract

$Pb(Mn_{1/3}Sb_{2/3})_{0.01}(Ni_{1/3}Nb_{2/3})_{0.495}(Zr_{0.3}Ti_{0.7})_{0.495}O_3$+x wt% Ta_2O_5 (PMS–PNN–PZT, x = 0, 0.2, 0.4, 0.6, 0.8) lead piezoelectric ceramics were prepared by a traditional two-step solid-state reaction method. The effect of Ta_2O_5 content on the phase structure, microstructure, electrical properties and dielectric relaxation of PMS–PNN–PZT ceramics was investigated. The XRD patterns show that all ceramics have pure perovskite structure. Ta_2O_5 doping can promote the grain growth and improve electrical properties. And the ceramics have high relaxation behavior. When x = 0.4, it exhibits optimum electrical performance: d_{33} = 805 pC/N, k_p = 66%, ε_r = 6838, tanδ = 1.4%, T_c = 118.5 °C, γ = 1.9618, E_c = 3.652 kV/cm, P_r = 21.91 μC/cm^2. This indicates that Ta_2O_5 can be used as an effective dopant in PMS–PNN–PZT ceramics and the ceramics can be used as the main material for multilayer ceramic capacitors and electro-strictive actuators.

1 Introduction

Lead based piezoelectric ceramics are widely used in national defense, information and communication, aerospace, navigation, medicine, bioengineering, agriculture and other fields [1–3]. In recent years, lead nickel niobate (PNN) based and lead zirconate titanate (PZT) based piezoelectric ceramics have been widely researched. $Pb(Ni_x, Nb_y)O_3$ are relaxor ferroelectrics with high dielectric constant and piezoelectric constant [4]. $Pb(Zr_x, Ti_y)O_3$ have high piezoelectric properties, especially at the morphotropic phase boundary (MPB). It has the advantages of convenient preparation and low cost [5]. At present, many scholars have studied how to improve the performance of piezoelectric ceramics for meeting the needs of social development. The performance of piezoelectric ceramics is improved by introducing elements and doping trace elements [6]. So, there are appearing some composite piezoelectric ceramic systems now. The main examples are as follows: $Pb(Ni_{1/3}Nb_{2/3})_x(Zr,Ti)_yO_3$ (PNN–PZT) [7], $Pb(Mg_{1/3}Nb_{1/3})O_3$–$Pb(Zr,Ti)O_3$ (PMN–PZT) [8], $Pb(Mn_{1/3}Sb_{2/3})O_3$–$PbZrO_3$–$PbTiO_3$ (PMS–PZT) [9], $Pb_{1-x}Ba_x(Zn_{1/2}Nb_{1/2})_y(Ni_{1/3}Nb_{2/3})_z(Zr,Ti)_{1-y-z}O_3$ (PZN–PNN–PZT–BZT) [10], $yPb(In_{1/2}Nb_{1/2})O_3$–$(1-x-y)Pb(Mg_{1/3}Nb_{2/3})O_3$-$xPbTiO_3$ (PIN–PMN–PT) [11], $PbHfO_3$–$PbTiO_3$–$Pb(Mg_{1/3}Nb_{2/3})O_3$ (PMN–PST) [12], $PbHfO_3$–$PbTiO_3$–$Pb(Mg_{1/3}Nb_{2/3})O_3$ (PMN–PHT) [13]. Meanwhile, PNN–PZT based piezoelectric ceramics are represented by high piezoelectric properties, but dielectric loss of the system is relatively high. PMS based ceramics are typical relaxor ferroelectrics with good piezoelectric properties, especially low dielectric loss. PMS–PNN–PZT piezoelectric ceramics were selected in this experiment. On the other way, in order to satisfy the requirement of different electrical products, many researchers try to achieve the desired requirements by doping trace elements.

The results show that appropriate doping of trace elements in lead based piezoelectric ceramics will improve their properties [14–16]. Ta_2O_5 is a kind of high-valence oxide. Some researchers doped it into the lead-free piezoelectric ceramics and studied the improvement of lead-free piezoelectric ceramics [17, 18]. Lin et al. [19] found that piezoelectric constant and electromechanical coupling coefficient are effectively improved by adding Ta^{5+} into the $K_{0.5}Na_{0.5}Nb_{1-x}Ta_xO_3$ system. Du et al. [20] reported that $BiFe_{0.5}Ta_{0.5}O_3$ doping into KNN system can

✉ De-Yi Zheng
zhengdeyi@hotmail.com

Hong-Wei Zhu
zrv941015@163.com

[1] College of Big Data and Information Engineering, Gui Zhou University, Guiyang 550025, China

[2] College of Materials and Metallurgy, Gui Zhou University, Guiyang 550025, China

[3] Guizhou Zhenhua Electronic Information Industry Technology Research Co., Ltd, Guiyang 550018, China

availably increase the grain size and improve piezoelectric performance.

But few researchers studied the effect of Ta^{5+} on the electrical properties of lead based piezoelectric ceramics. Ta^{5+} and Nb^{5+} have similar chemical properties. Doping Nb^{5+} can improve electrical properties [21]. So, Ta_2O_5 was introduced into 0.01PMS–0.495PNN–0.495PZT ceramics to study effects of Ta^{5+} additive on the phase structure, microstructure, electric properties and relaxation behavior in this paper. The results show that addition of Ta_2O_5 effectively improves the piezoelectric performance. Moreover, the ceramics exhibit obvious dielectric relaxation behavior. It is indicated that the PMS–PNN–PZT + xTa^{5+} piezoelectric ceramics can be applied at multilayer ceramic capacitors and electro-strictive actuators.

2 Experimental procedure

$Pb(Mn_{1/3}Sb_{2/3})_{0.01}(Ni_{1/3}Nb_{2/3})_{0.495}(Zr_{0.3}Ti_{0.7})_{0.495}O_3$+x wt% Ta_2O_5 (x = 0, 0.2, 0.4, 0.6, 0.8) piezoelectric ceramics were synthesized by traditional solid sintering method. The raw materials are analytical-grade metal oxides powders: Pb_3O_4(99.0%), ZrO_2(99.5%), TiO_2(99.6%), Nb_2O_5(99.5%), Ni_2O_3(99.0%), MnO_2(99.0%), Sb_2O_3 (99.0%) and Ta_2O_5(99.99%). Firstly, each raw material needed to be calculated according to the chemical formula and measured with a balance. In order to compensate for the volatilization of Pb during sintering process, the Pb_3O_4 weighed with excess 1 wt%. Then the mixture was placed a ball mill with alcohol. The purpose of adding alcohol was to make the powder more refined. The mixtures were ball-milled in alcohol for 10 h. The ball milled materials were dried and then burned for 4 h at 920 °C. The calcined powders were ball-milled again for 10 h. After drying, the powders were pressed into tablets with 6 wt% paraffin waxes under 5 MPa with the size of ϕ12 mm × 1 mm. Subsequently, samples were placed in a sintering furnace and sintered for 2 h at 1260 °C under closed conditions. The heating rate was 2 °C per minute. Then samples were cooled down to room temperature with the furnace.

The crystal phase composition of samples was measured by using an X-ray diffractometer (XRD, Model Panalytical/X'pert-PRO, Holland). The cross-sectional microstructure of specimens was observed by scanning electron-microscopy (SEM, Model SUPRA40, Germany). Samples were applied silver paste on both sides and heated for 20 min at 700 °C. Then they were poled in silicon oil at 50 °C under DC electric field of 2 kV/mm for 30 min. The piezoelectric constants of ceramics were determined by using a quasi-static d_{33} meter (ZJ-3A; Institute of Acoustics Academic Science, China). The electromechanical coupling coefficients (k_p) were calculated by resonance and anti-resonance techniques using an electric oscillator (Model UX21) under 1 kHz. The relative permittivity and dielectric loss as functions of temperature were evaluated with an LCR meter (TZDM system), which connects to a computer-controlled temperature chamber. The test frequencies range from 1 kHz to 1 MHz. According to the following formula [22, 23]:

$$k_p = \sqrt{2.54 \times \frac{(f_p - f_s)}{f_s}} \tag{1}$$

$$\varepsilon_r = \frac{\varepsilon}{\varepsilon_0} = \frac{Cd}{\varepsilon_0 S} = \frac{4Cd}{\varepsilon_0 \pi \phi^2} \approx \frac{144Cd}{\phi^2} \tag{2}$$

The free space dielectric constant value ε_0 is 8.85×10^{-12} F/m, C denotes capacitance (units 10^{-12} F), d denotes the sample thickness (mm), S denotes the area (mm^2), ϕ denotes the sample diameter.

$$Q_m = f_a{}^2[2\pi R_f C f_r(f_a{}^2 - f_r{}^2)]^{-1} \tag{3}$$

The f_r is resonance frequency (Hz), f_a is antiresonance frequency (Hz). Q_m is the minimum impedance at f_r (ohm) resonance impedance, C is capacitance mechanically free at 1 kHz.

3 Results and discussion

After samples preparation, the conclusions of X-ray diffraction, scan electron-microscopy, piezoelectric, dielectric and ferroelectric properties have been done for evaluating the quality of PMS–PNN–PZT based piezoelectric ceramics.

3.1 Phase structure of ceramic

Figure 1a shows the X-ray diffraction (XRD) patterns of 0.01PMS–0.495PNN–0.495PZT ceramics with different Ta_2O_5 content sintered at 1260 °C. In the Fig. 1a, no detectable secondary phase peak can be found, which indicates that all the samples are pure perovskite structure. It proves that Ta^{5+} diffused into the lattice and fused with the substrate to form a solid solution. Figure 1b shows the magnified XRD patterns of ceramics in the range of 44–46°. It can be clearly observed that location of peaks changes with increase of Ta_2O_5 amount, the diffraction peak near the 45° shifts to lower angles. With Ta_2O_5 doping, elements substitution occurs in the system. According to the principle of ionic radius similarity, when Ta^{5+} doped into the main lattice of the system, it will give priority to the substitution of B-site ion. So, it makes the lattice constant of crystal larger and the diffraction peak offsets to the lower angle. This phenomenon indicates that doping Ta^{5+} not only causes

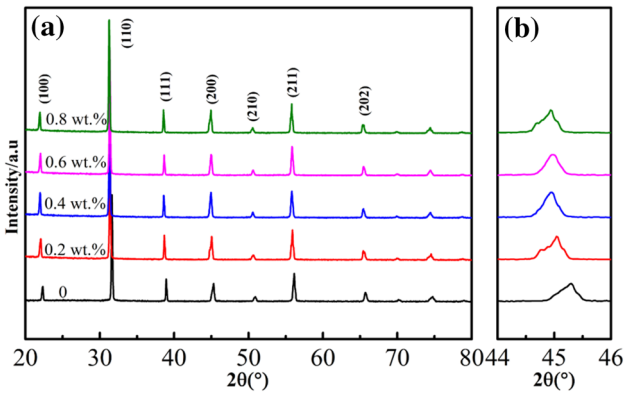

Fig. 1 X-ray diffraction patterns of 0.01PMS–0.495PNN–0.495PZT+x wt% Ta_2O_5 ceramics

lattice distortion, but also changes the phase composition of samples. All samples exhibit the tetragonal phase structure without phase structure transformation.

3.2 Sectional microstructure of ceramics

Figure 2 shows the SEM images of the PMS–PNN–PZT+x wt% Ta_2O_5 (x = 0, 0.2, 0.4, 0.6, 0.8) ceramics sintered at 1260 °C for 2 h. It can be seen from Fig. 2 that when moderate amount of Ta_2O_5 was doped, the grains inside the ceramics become full, and the grain size distribution is more uniform. At x = 0.4, the structure is the most compact. At this point, it exhibits optimum electrical performance value. However, there are many fine grains when x > 0.4. This is due to excessive Ta^{5+} concentrate on the grain boundary without entering the lattice and forming a solid solution. The specific surface area between the fine grains is increased. The dislocation will tangle at the grain boundary, which hinders the motion of the domain. And it has the clamping effect on the domain [24]. So, polarization of the domain is difficult and electrical properties become worse.

3.3 Electrical properties of ceramics

Figure 3 shows the electrical properties of PMS-PNN-PZT+x wt% Ta_2O_5 ceramics. In the Fig. 3a, it can be seen that the Ta^{5+} doping can effectively improve performance of the piezoelectric ceramics. With the increase of Ta^{5+} doping, the piezoelectric constant (d_{33}) and the electromechanical coupling coefficient (k_p) have different degrees of improvement. When the amount of doping is 0.4 wt%, d_{33} and k_p show the maximum values. It is due to the increase of the lattice constant caused by doping, resulting in an increase in the electrical dipole moment. B-site ions are further away from the center. So, the piezoelectric performance is improved. In the other hand, due to the occurrence of high-valent ion substitution, cation vacancies are formed, which improves the mobility of the crystal structure. Thereby promoting the deflection of the domain, the ceramic sample is more polarized. The d_{33} and k_p values are effectively improved.

In the Fig. 3b, the ε_r value increases with increase of Ta^{5+} content. It may be that the incorporated Ta^{5+} replaces Mn^{2+}.

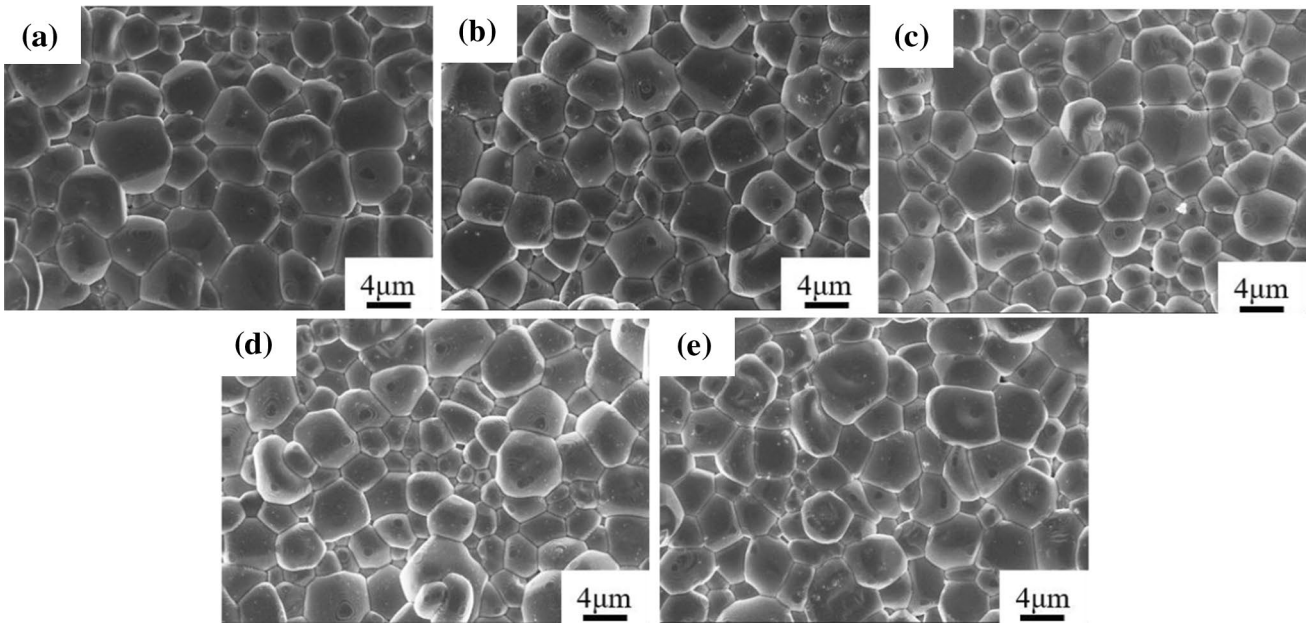

Fig. 2 Sectional microstructure of 0.01PMS–0.495PNN–0.495PZT+x wt% Ta_2O_5 ceramics. **a** x = 0, **b** x = 0.2, **c** x = 0.4, **d** x = 0.6, **e** x = 0.8

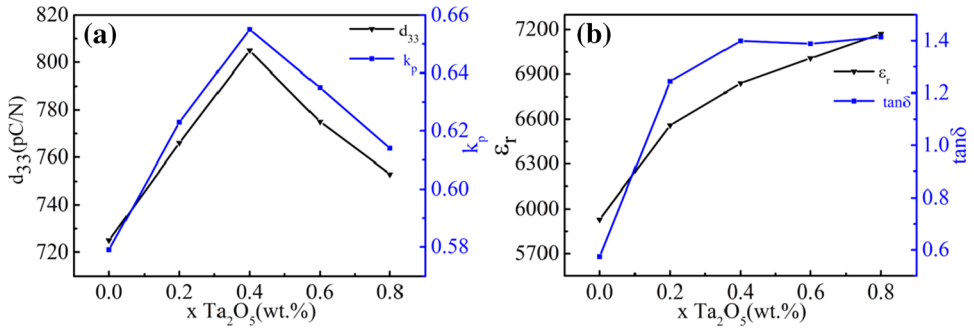

Fig. 3 **a** d_{33} and k_p, **b** ε_r and tanδ properties of the 0.01PMS–0.495PNN–0.495PZT + x wt% Ta_2O_5 ceramics

Mn^{2+} ions can effectively reduce ε_r values of system [25]. The dielectric constant gradually increases when content of Mn^{2+} ions decreases in this system. For the change of tanδ value, it is probable that substitution of high-valent ions makes the electrovalency unbalance. This system forms the cation vacancy, which is beneficial to the motion of domain boundary. The tanδ value begins to increase gradually. However, when the content of Ta^{5+} ions is more than 0.4 wt%, change of tanδ is not obvious. Excessive Ta^{5+} ions stockpile at the grain boundary, make the domain boundary deflection more difficult. Thus, the tanδ value does not increase further.

3.4 Dielectric properties of ceramics

Figure 4a shows temperature dependence of the dielectric constant for PMS–PNN–PZT + x wt% Ta_2O_5 ceramics at the frequency of 10 kHz. The test temperature ranges from room temperature to 280 °C. Figure 4b is the Curie temperature at 10 kHz. It can be seen from the Fig. 4 that the Curie temperature (T_c) decreases with increase of Ta^{5+} content. T_c value of piezo-ceramic materials reflects the difficulty of B-bite ions deviating from the center position in BO_6 oxide octahedral. Because of increase of lattice constant caused by ion-doping, the distance between B-site ions and oxygen ions will increase. As the distance increases, the interaction between the B-site ions and oxygen ions weakens and transition energy of phase structure will be reduced. So, T_c decreases with increase of Ta^{5+} content. It is shown from Fig. 4a that the maximum permittivity of the dielectric constant increases with increase of Ta^{5+} content and no other peaks are found from room temperature to 280 °C. The results also show that there is no transition from rhombohedral to tetragonal phase in this system. It is in accordance with the results of the XRD graph analysis.

3.5 Relaxation behavior of ceramics

Figure 5 shows the inverse dielectric constant as a function of temperature for 0.01PMS–0.495PNN–0.495PZT + x wt% Ta_2O_5 ceramics at 10 kHz. For normal ferroelectrics, when temperature is higher than the Curie temperature, dielectric permittivity should follow the Curie–Weiss law described by Ref. [26]:

$$\frac{1}{\varepsilon} = \frac{T - T_{CW}}{C} \tag{4}$$

where C is the Curie–Weiss constant and T_{cw} is the Curie–Weiss temperature. The T_{cw} can be obtained by formula (4). Through the Fig. 5 can observe the relationship between dielectric constant and temperature, it does not follow the Curie–Weiss formula. The degree of the deviation from the Curies–Weiss law is defined by ΔT_m as formula (5) [27]:

$$\Delta T_m = T_B - T_m \tag{5}$$

T_B is the initial temperature where the dielectric constant conforms to Curie's law and T_m is corresponding

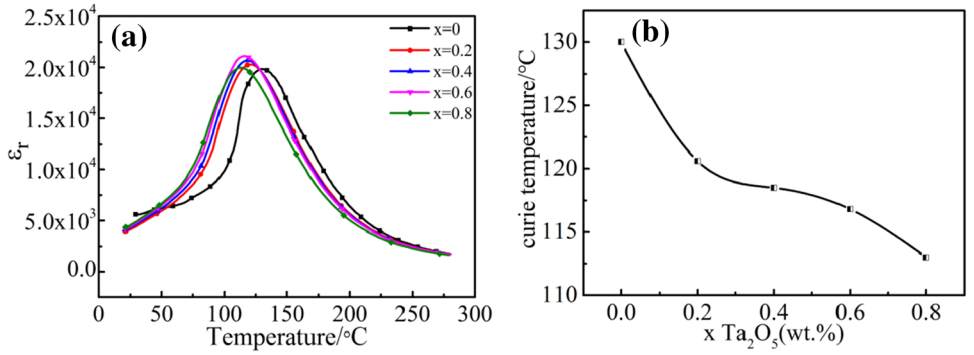

Fig. 4 Temperature dependence of **a** dielectric constant ceramics at 10 kHz, **b** Curie temperature

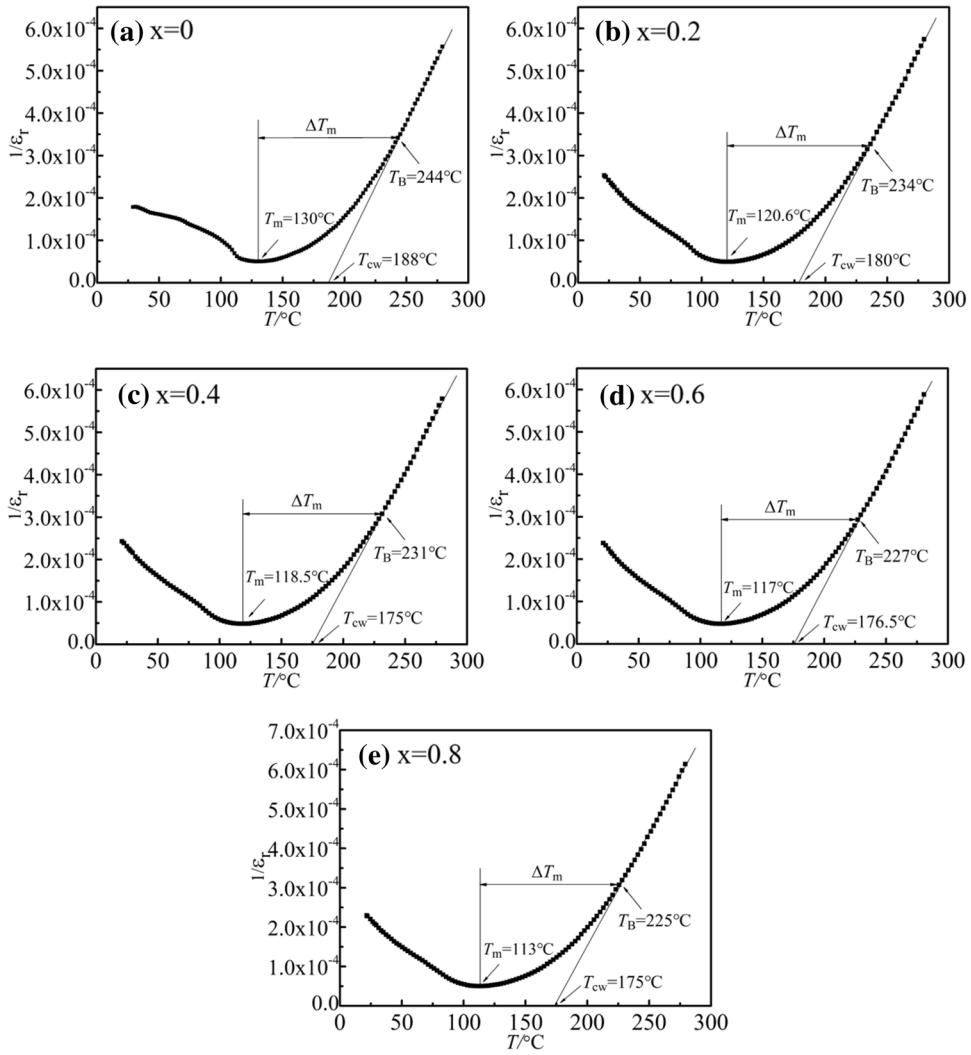

Fig. 5 The inverse dielectric constant at 10 kHz as a function of temperature for the 0.01PMS–0.495PNN–0.495PZT + x wt% Ta_2O_5 ceramics

temperature of the maximum dielectric constant. Table 1 shows some values about dielectric properties. From the Table 1, there is no obvious change about ΔT_m with increase of Ta^{5+} content. It indicates that the dielectric relaxation of all samples is relatively close.

For the relaxation ferroelectric, it can be studied according to the modified Curie–Weiss law [28–30]:

$$\frac{1}{\varepsilon} - \frac{1}{\varepsilon_m} = \frac{(T - T_m)^\gamma}{C_1}, \quad (T > T_m,\ 1 \le \gamma \le 2) \tag{6}$$

where C_1 is the Curie constant, ε_m and T_m are the maximum dielectric constant and temperature correspondingly, γ is called a diffusion coefficient ranging from 1 (normal ferroelectric) to 2 (complete relaxor ferroelectric). Figure 6 shows that plot of $\ln(1/\varepsilon_r - 1/\varepsilon_m)/\ln(T - T_m)$ at 10 kHz for ceramics. Figure 6f is the variation of dispersion coefficient of Ta^{5+} ceramics doped with different contents and the dispersion coefficient (γ) is fitted by formula (6). The dispersion values of all samples are > 1.90, indicating that they have obvious dielectric relaxation behavior. With increase of Ta^{5+} content, the dispersion coefficient has hardly changed,

Table 1 Summary of some parameters extracted from ceramics dielectric measurements at 10 kHz

x	T_{cw}/°C	T_B/°C	T_m/°C	ΔT_m/°C	ε_m (10 kHz)	γ
0	188	244	130	114	14,174	1.9937
0.2	180	234	115	114.5	20,302	1.9987
0.4	175	231	118.5	112.5	20,706	1.9618
0.6	176.5	227	117	110	21,122	1.9189
0.8	175	225	113	112	19,990	1.9905

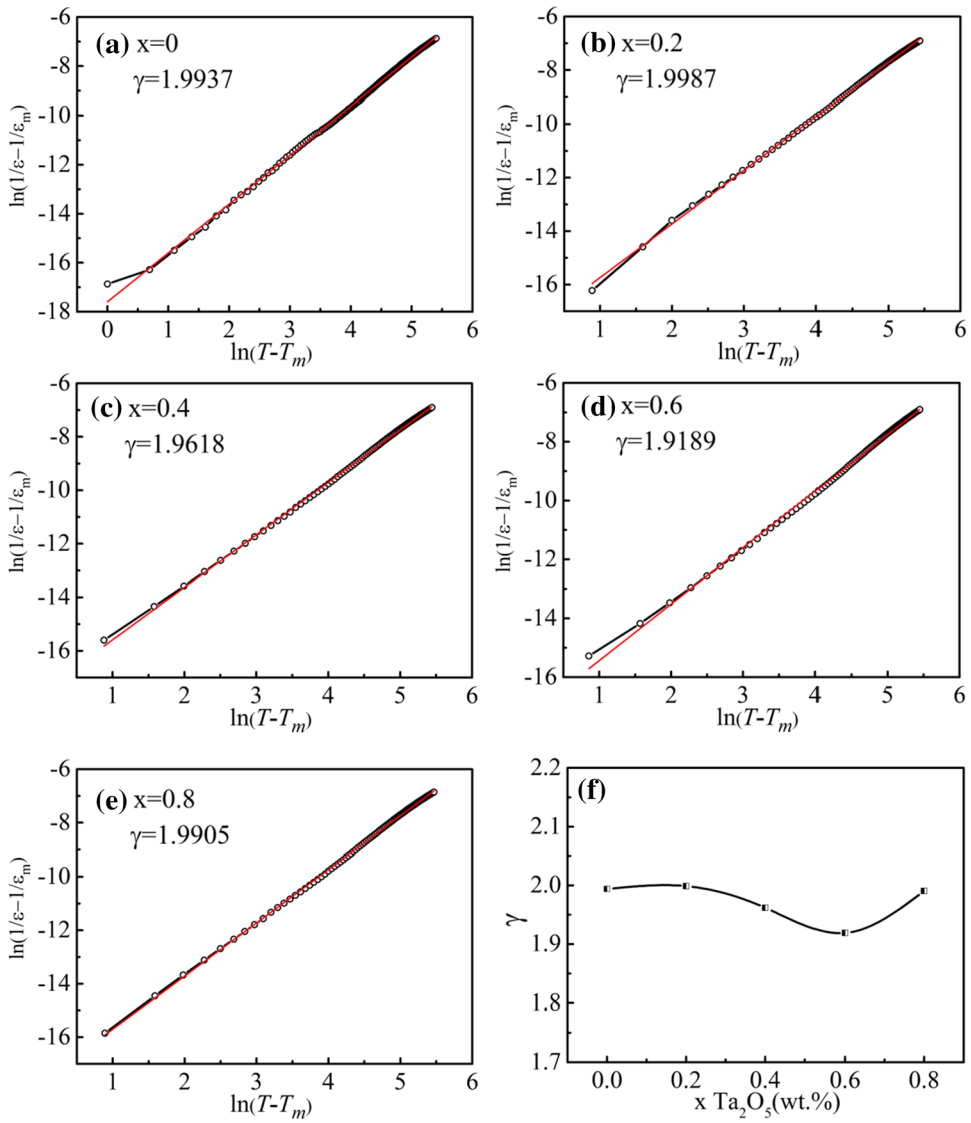

Fig. 6 Plot of $\ln(1/\varepsilon - 1/\varepsilon_m)/\ln(T - T_m)$ at 10 kHz for 0.01PMS–0.495PNN–0.495PZT + x wt% Ta_2O_5 ceramic samples

indicating that doping in this range will not affect dielectric relaxation degree of this system.

3.6 Ferroelectric behavior of ceramics

Figure 7a shows P–E hysteresis loops of samples with different Ta_2O_5 content. Figure 7b shows remnant polarization (P_r) and coercive field (E_c) of samples. From Fig. 7, all

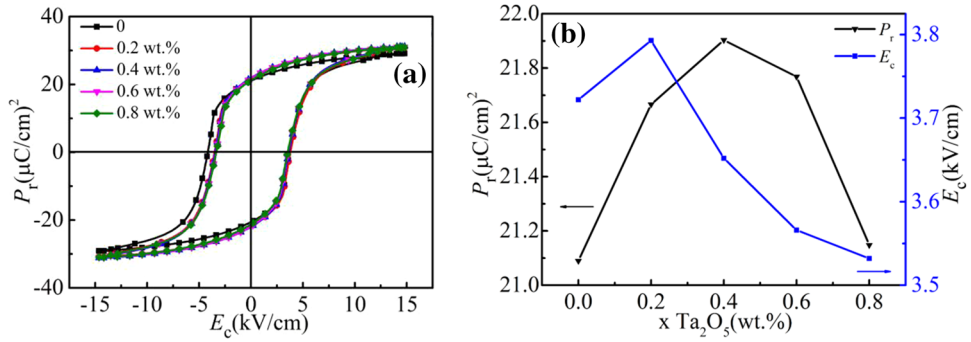

Fig. 7 **a** P–E hysteresis loops and **b** P_r and E_c for 0.01PMS–0.495PNN–0.495PZT + x wt% Ta_2O_5 samples

samples show typical ferroelectric hysteresis loops. With increase of Ta_2O_5 content, the remnant polarization (P_r) and the coercive field (E_c) increase first and then decrease. But the changes are not obvious. When x = 0.4, P_r reaches the maximum value (21.91 μC/cm^2) and E_c value is smaller, which is 3.652 kV/cm. In addition, the hysteresis loop is the fullest and the polarization is the most sufficient, which further verifies the change of electrical properties. To sum up, it is suggested that Ta_2O_5 doping can strengthen the ferroelectric properties of the ceramics.

4 Conclusions

In conclusion, $Pb(Mn_{1/3}Sb_{2/3})_{0.01}(Ni_{1/3}Nb_{2/3})_{0.495}(Zr_{0.3}Ti_{0.7})_{0.495}O_3$+x wt% Ta_2O_5 (PMS–PNN–PZT, x = 0, 0.2, 0.4, 0.6, 0.8) lead piezoelectric ceramics were prepared by a traditional two-step solid-state reaction method. The effects of Ta_2O_5 on the phase structure, micro-structure, electrical properties and relaxation behavior of the ceramics were systematically studied. The result of XRD diagram shows that all samples are pure perovskite structure. They all show obvious dielectric relaxation behavior. The dispersion coefficient value almost does not change, indicating that incorporation of Ta^{5+} does not affect the degree of dielectric relaxation in the system. When x = 0.4, it exhibits optimum electrical performance: d_{33} = 805 pC/N, k_p = 66%, ε_r = 6838, tanδ = 1.4%, T_c = 118.5 °C, γ = 1.9618, E_c = 3.652 kV/cm, P_r = 21.91 μC/cm^2. These results confirm that the ceramic is with the potentialities to be applied in multilayer ceramic capacitors and electro-strictive actuators.

Acknowledgements The authors acknowledge the support of project of Guizhou Provincial Education Department (QJH KY Z [2017]001) and Guizhou Provincial Science and Technology Department (QKH LH Z [2017]7248).

References

1. R. Cao, G. Li, J. Zeng et al., The Piezoelectric and dielectric properties of 0.3Pb($Ni_{1/3}Nb_{2/3}$)O_3-x$PbTiO_3$-(0.7-x)$PbZrO_3$ ferroelectric ceramics near the morphotropic phase boundary. J. Am. Ceram. Soc. **93**(3), 737–741 (2010)
2. W.P. Chu, C.P. Chong, C.K. Liu et al., Placement of piezoelectric ceramic sensors in ultrasonic wire-bonding transducers. Microelectron. Eng. **66**(1), 750–759 (2003)
3. Z.H. Peng, D.Y. Zheng, T. Zhou et al., Effects of Co_2O_3 doping on electrical properties and dielectric relaxation of PMS-PNN-PZT ceramics. J. Mater. Sci. Mater. Electron. **5**, 1–8 (2018)
4. G.G. Peng, D.Y. Zheng, S.M. Hu et al., Effects of rare-earth Sm_2O_3 addition on relaxation behavior and electric properties of 0.5PNN-0.5PZT ceramics. J. Mater. Sci. Mater. Electron. **27**(6), 5509–5516 (2016)
5. T. Stevenson, D.G. Martin, P.I. Cowin et al., Piezoelectric materials for high temperature transducers and actuators. J. Mater. Sci. Mater. Electron. **26**(12), 9256–9267 (2015)
6. Q. Liao, X. Chen, X. Chu et al., Effect of Fe doping on the structure and electric properties of relaxor type BSPT-PZN piezoelectric ceramics near the morphotropic phase boundary. Sensors Actuators A Phys **201**(10), 222–229 (2013)
7. E.F. Alberta, A.S. Bhalla, Piezoelectric and dielectric properties of transparent Pb($Ni_{1/3}Nb_{2/3}$)1-x-y$Zr_xTi_yO_3$ ceramics prepared by hot isostatic pressing[J]. Int. J. Inorg. Mater. **3**(01), 987–995 (2015)
8. S. Fujii, E. Fujii, R. Takayama et al., Preparation of Pb($Mg_{1/3}Nb_{2/3}$)O_3-Pb(Zr,Ti)O_3 thin films by RF-magnetron sputtering and their electrical and piezoelectric properties. Jpn. J. Appl. Phys. **48**(1), 015502–015502 (2009)
9. K. Brajesh, A.K. Himanshu, H. Sharma et al., Structural, dielectric relaxation and piezoelectric characterization of Sr^{2+} substituted modified PMS-PZT ceramic. Phys B Condens. Matter **407**(4), 635–641 (2012)
10. T. Yu, G. Zhang, Y. Yu et al. Pyroelectric energy harvesting devices based-on Pb[(Mn_xNb_{1-x})$_{1/2}$(Mn_xSb_{1-x})$_{1/2}$]$_y$(Zr_zTi_{1-z})$_{1-y}O_3$ ceramics. Sensors Actuators A Phys, **223**, 159–166 (2015)
11. D. Wang, M. Cao, S. Zhang, Phase diagram and properties of Pb($In_{1/2}Nb_{1/2}$)O_3-Pb($Mg_{1/3}Nb_{2/3}$)O_3-$PbTiO_3$ polycrystalline ceramics. J. Eur. Ceram. Soc. **32**(2), 433–439 (2012)
12. D. Wang, M. Cao, S. Zhang, Investigation of ternary system $PbHfO_3$-$PbTiO_3$-Pb($Mg_{1/3}Nb_{2/3}$)O_3 with morphotropic phase boundary compositions. J. Am. Ceram. Soc. **95**(10), 3220–3228 (2012)
13. Y. Li, D. Wang, W. Cao et al., Effect of MnO_2 addition on relaxor behavior and electrical properties of PMNST ferroelectric ceramics. Ceram. Int. **41**(8), 9647–9654 (2015)
14. D. Wang, J. Li, M. Cao et al., Effects of Nb_2O_5 additive on the piezoelectric and dielectric properties of PHT-PMN ternary ceramics near the morphotropic phase boundary. Phys Status Solidi **211**(1), 226–230 (2014)
15. D. Wang, Q. Zhao, M. Cao et al., Dielectric, piezoelectric, and ferroelectric properties of Al_2O_3 and MnO_2 modified $PbSnO_3$-$PbTiO_3$-Pb($Mg_{1/3}Nb_{2/3}$)O_3 ternary ceramics. Phys Status Solidi **210**(7), 1363–1368 (2013)
16. Y. Li, J. Yuan, D. Wang et al., Effects of Nb, Mn doping on the structure, piezoelectric, and dielectric properties of 0.8Pb($Sn_{0.46}Ti_{0.54}$)O_3-0.2Pb($Mg_{1/3}Nb_{2/3}$)O_3 piezoelectric ceramics. J. Am. Ceram. Soc. **96**(11), 3440–3447 (2013)
17. F. Rubio-Marcos, J.F. Fernandez, D.A. Ochoa et al., Understanding the piezoelectric properties in potassium-sodium niobate-based lead-free piezoceramics: interrelationship between intrinsic and extrinsic factors. J. Eur. Ceram. Soc. **37**(11), 3501–3509 (2017)
18. F. Zeng, Q. Liu, E. Cai et al., Relaxor phenomenon of (1-x)($Ba_{0.85}Ca_{0.15}$)($Zr_{0.09}Ti_{0.91}$)O_3-xTa+ 0.6wt.%Li_2CO_3, ceramics with high piezoelectric constant and Curie temperature. Ceram. Int. **44**, 10677–10684 (2018)
19. D. Lin, K.W. Kwok, H.L.W. Chan, Phase transition and electrical properties of ($K_{0.5}$ $Na_{0.5}$)($Nb_{1-x}Ta_x$)O_3 lead-free piezoelectric ceramics. Appl. Phys. A **91**(1), 167–171 (2008)
20. J. Du, F. An, Z. Xu et al., Effects of $BiFe_{0.5}Ta_{0.5}O_3$ addition on electrical properties of $K_{0.5}Na_{0.5}NbO_3$ lead-free piezoelectric ceramics. Ceram. Int. **42**(1), 1943–1949 (2016)
21. M. Pereira, A.G. Peixoto, M.J.M. Gomes, Effect of Nb doping on the microstructural and electrical properties of the PZT ceramics. J. Eur. Ceram. Soc. **21**(10–11), 1353–1356 (2001)
22. G.G. Peng, D.Y. Zheng, C. Cheng et al., Effect of rare-earth addition on morphotropic phase boundary and relaxation behavior of the PNN-PZT ceramics. J. Alloys Compds. **693**, 1250–1256 (2017)
23. J. Ji, B. Fang, X. Zhao et al., Effects of nano-sized BCZT on structure and electrical properties of KNN-based lead-free piezoceramics. J. Mater. Sci. Mater. Electron. **29**(6), 1–10 (2017)

24. Z. LI, L. ZHANG, X. YAO, Dielectric properties anomaly of (1-*x*) $Pb(Ni_{1/3}Nb_{2/3})$-*x*$PbTiO_3$ ceramics near the morphotropic phase boundary. J. Mater. Res. **16**(3), 834–836 (2001)
25. Y. Yu, J. Wu, T. Zhao et al., MnO_2 doped PSN-PZN-PZT piezoelectric ceramics for resonant actuator application. J. Alloys Compds. **615**(31), 676–682 (2014)
26. H. Cheng, H. Du, W. Zhou et al., $Bi(Zn_{2/3}Nb_{1/3})O_3$-$(K_{0.5}Na_{0.5})NbO_3$ high-temperature lead-free ferroelectric ceramics with low capacitance variation in a broad temperature usage range. J. Am. Ceram. Soc. **96**(3), 833–837 (2013)
27. N. Pisitpipathsin, P. Kantha, K. Pengpat et al., Influence of Ca substitution on microstructure and electrical properties of Ba(Zr,Ti)O_3 ceramics. Ceram. Int. **39**(2), S35–S39 (2013)
28. R. Nie, Q. Zhang, Y. Yue et al., Properties of low-temperature sintering PNN-PMW-PSN-PZT piezoelectric ceramics with $Ba(Cu_{1/2}W_{1/2})O_3$ sintering aids. Int. J. Appl. Ceram. Technol. **13**(6), 1119–1124 (2016)
29. M. Promsawat, A. Watcharapasorn, Z. Ye et al., Enhanced dielectric and ferroelectric properties of $Pb(Mg_{1/3}Nb_{2/3})_{0.65}Ti_{0.35}O_3$ ceramics by ZnO modification. J. Am. Ceram. Soc. **98**(3), 848–854 (2015)
30. C. Lei, K.P. Chen, X.W. Zhang et al., Study of the structure and dielectric relaxation behavior of $Pb(Ni_{1/3}Nb_{2/3})$-$PbTiO_3$ ferroelectric ceramics. Solid State Commun. **123**(10), 445–450 (2002)